JOURNAL OF GEOPHYSICAL RESEARCH, VOL. 94, NO. B6, PAGES 7332–7342, JUNE 10, 1989

A Paleomagnetic Constraint on the Late Cretaceous Paleoposition of Northwestern Baja California, Mexico

P. E. FILMER

Department of Earth, Atmospheric, and Planetary Sciences, Massachusetts Institute of Technology, Cambridge

J. L. KIRSCHVINK

Division of Geological and Planetary Sciences, California Institute of Technology, Pasadena

We present palaeomagnetic data for Cretaceous sedimentary rocks from the El Rosario formation of northwestern Baja California which imply a northward displacement of 15.0 ± 3.8° and a 30.8 ± 4.2° clockwise rotation for the Baja Peninsula relative to the North American craton since Late Cretaceous time. Paired IRM acquisition, X-ray diffraction, and Mössbauer spectra indicate that fine-grained magnetite is the dominant magnetic mineral present, with goethite and other more oxidized phases rare to absent. Biochemical evidence constrains the amount of diagenesis undergone by the sediments. We subjected oriented samples to both progressive alternating field and thermal demagnetization, and in general found univectorial magnetizations, yielding a mean inclination of 44.6° and declination of 5.3° with an α_{95} of 2.0°. The corresponding paleolatitude for these values is 26.3 ± 1.6°. Most of the samples were of normal polarity, which is consistent with their deposition within the upper Campanian chron 33N. We collected samples from younger Maastrichtian sediments which yield consistent, reversed directions.

INTRODUCTION

Current debates on the tectonics of the Baja California Peninsula focus on the geological, geochronological, and paleomagnetic data. Whereas the geological and geochronological data seem to indicate a motion since the Cretaceous of between 300 and 500 km to the north [*Beck and Plumley*, 1979; *Page*, 1981; *Gastil et al.*, 1975, 1981], paleomagnetic data indicate a much larger motion, involving 1200 km of motion for the peninsula [*Patterson*, 1984; *Fry et al.*,1985; *Hagstrum et al.*, 1985; *Champion et al.*, 1986]. Similar magnitudes of displacement and rotation have been observed in the Southern California Batholith province [*Teissère and Beck*, 1973]. These results are summarized in Table 1, and the sampling site locations are illustrated in Figure 1. We present an extensive body of results from a site in northwestern Baja California that support a northward translation of 15° and a clockwise rotation of 31° for this particular area of the peninsula.

Displaced terranes pose inherently difficult problems for the interpretation of paleomagnetic data. The terranes often have complex geologic histories, and the rocks riding on them have possibly acquired several different components of remanent magnetism, making the paleomagnetic interpretation difficult and often ambiguous. In particular, the paleomagnetic poles from Cretaceous sedimentary rocks in the Baja California Peninsula fall perilously close to the present field direction, making recent remagnetization a valid suspicion. Our approach to this problem has been to focus on the exceptionally well-preserved sediments of the El Rosario formation [*Kilmer*, 1965; *Gastil et al.*, 1975]. These sediments are widely exposed in the Northwestern portion of the Baja California Peninsula, where, along the coast, they form seacliffs that range from 3 to 15 m in height.

Several lines of evidence suggest that the grey-green facies of the El Rosario formation has been subjected to a minimum of diagenetic chemical or thermal alteration, and hence should be free of chemoremanent or thermoremanent magnetic overprints. First, the sedimentary rocks contain numerous, well-preserved molluscan fossils, including ammonites, gastropods, and pelecypods. In particular, the calcium carbonate within the ammonites is preserved in the original, less stable aragonite form [*Weiner and Lowenstam*, 1980], which still retains its pearly luster. The presence of the aragonite phase of calcium carbonate has been recognized as an indication of no more than mild diagenesis [*Bøggild*, 1930; *Curtis and Krinsley*, 1965]. The dry polymorphic inversion of aragonite at 25°C may take tens of millions of years, while the wet inversion is a catalyzed process, with 100% inversion occurring within 30 hours in 0.01M NaCl at 1 atmosphere and 66°C, and within 50 hours for pure water at 1 atmosphere and 108°C [*Bischoff and Fyfe*, 1968; *Jackson and Bischoff*, 1971; *Bathurst*, 1975; *Brand and Morrison*, 1987]. Since the aragonite phase is slightly more dense than the calcite phase, burial will retard the inversion. *Weiner and Lowenstam* [1980] examined the ultrastructure of the shells intensively and found that the original shell layers had been preserved on a submicron level. They found no infilling of boreholes, and no evidence of cementation or recrystallization. In addition, they found that the trace element concentration from fossil to fossil was similar, but was distinct from the clay matrix. The δ-O^{18} values led Weiner and Lowenstam to conclude that there had been minimal exchange with ground water, although they did not discount the possibility of anomalous local temperatures and δ-O^{18} values.

Second, *Weiner et al.* [1979], extended the studies of the aragonitic material to include the organic matrices, and found that while the matrix itself had been extensively altered, material of

Paper number 89JB00453.
0148–0227/89/89JB–00453$05.00

TABLE 1. Paleomagnetic Displacements for Various Localities

Locality	Age	N	I	D	κ	α_{95}	d	r	Paleolat	Reference
PSJ and PBS	uKr	112	44.6	5.3	28.8	2.0	15.0 ± 3.8	30.8 ± 4.2	26.3 ± 2.0	this study
Baja Average	Kr	50	–	–	263	3.4	10.9 ± 3.8	32.0 ± 4.5	26.7 ± 2.7	*Hagstrum et al.* [1985]
San Miguel Island	Kr	94	43.9	24.1	31.7	3.9	19.3	50.0 ± 5.7	25.7	*Champion et al* [1986]
Pigeon Point	uKr	63	-34.4	198.2	16.1	4.6	–	–	21.2 ± 5.3	*Champion et al.*[1984]
Santa Ana Mountains	uKr	80	45.1	323.6	–	6.7	17	-10	26.6	*Fry et al.*[1985]
Southern California Batholith	mKr	101	49.5	3.	48.5	5.0	–	–	–	*Teissèrre and Beck*[1973]

N, number of samples; I,D, average inclination and declination; κ, precision parameter; α_{95}, radius of circle of 95% confidence; d,r, poleward displacement and rotation, as explained in the text; Paleolat, latitude relative to a dipolar, coaxial, geocentric Kr pole [*Irving and Irving*, 1982].

low molecular weight was preserved essentially unaltered. They were able to determine that while some fraction of the matrix was lost, the low molecular weight fraction behaved comparably with weight fractions extracted from extant molluscan shells of the same superfamily in an ion exchange chromatography experiment. *Weiner et al.* [1979] concluded that the primary, secondary, and possibly even the tertiary conformations of some fraction of the molecules had been preserved. Diagenesis has therefore not been severe enough to fully denature the shell matrix proteins.

Finally, a more stringent constraint was placed on diagenesis by *Weiner and Lowenstam* [1980]. They discovered that the organic shell matrix contained no measurable amount of alloisoleucine epimer. The isoleucine had therefore not undergone the optical L-isoleucine to D-alloisoleucine epimerization reaction which is the basis of the amino acid racemization clock [*Hare and Abelson*, 1968; *Bada and Schroeder*, 1972]. Amino acids from Recent *Mercenaria* shells were completely racemized within one week at 160°C, at 1 atmosphere [*Hare and Abelson*, 1968]. The lack of epimerization for the *Baculites inornatus* in the intervening 63 Ma, when the characteristic epimerization time is about 10^5 years, is thought to be due to the stabilization of the amino acids by the bioinorganic phase of the shell matrix [*Weiner and Lowenstam*, 1980].

From these mineralogical and biochemical observations we

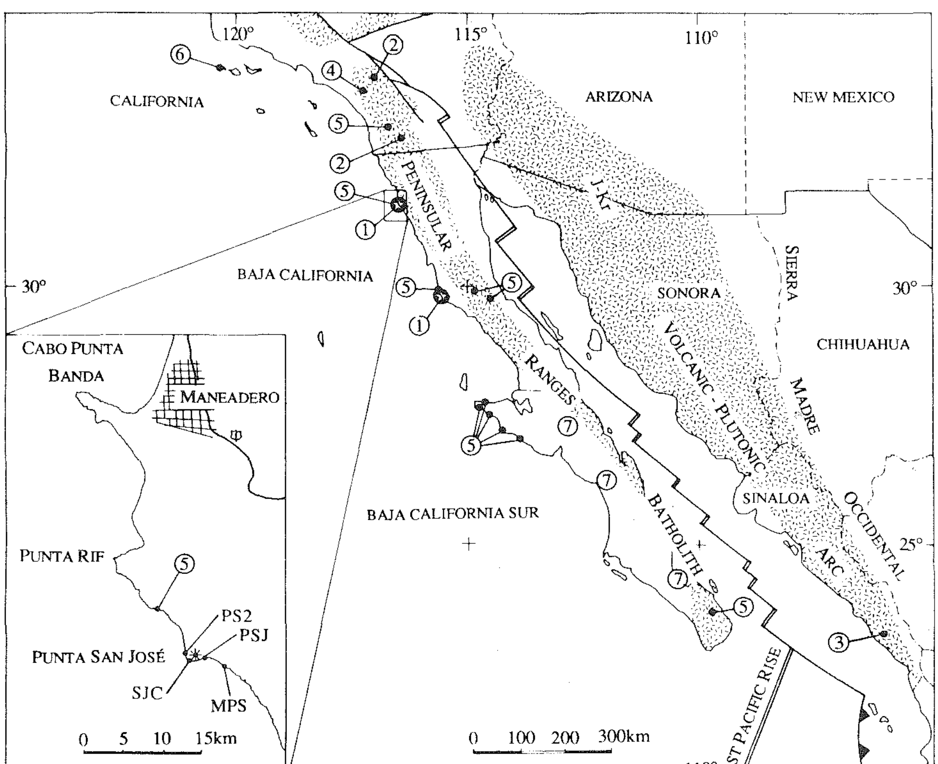

Fig. 1. Map of the Baja California Peninsula and the western Mexican mainland showing regional tectonic features. Dots indicate location of paleomagnetic sampling, and numbers indicate references: 1, this work; 2, *Teissère and Beck* [1973]; 3, *Bobier and Robin* [1973]; 4, *Fry et al.* [1985]; 5, *Hagstrum et al.* [1985]; 6, *Champion et al.* [1986]; and 7, *Hagstrum et al.* [1987]. Stippling indicates approximate locus of Jurassic and Cretaceous magmatic activity (after *Hagstrum et al.*, 1985, Figure 1) Inset: detail of sampling sites at Punta San José. Small dots indicate location of sites near the lighthouse. Site 5 is the location of the *Hagstrum et al.* [1985] Punta China site.

may reasonably infer that the thermal and chemical processes that often generate secondary magnetic components in paleomagnetic samples have not operated within the grey-green facies.

SITE DESCRIPTIONS

At Punta San José, sediments of the El Rosario formation were deposited within a local embayment of the Late Cretaceous sea which lapped onto tilted and deformed volcanogenic rocks of the mid-Cretaceous (Aptian-Albian) Alisitos formation. Over most of their exposed area, rocks of the El Rosario formation are poorly fossiliferous, and have a light reddish to reddish-orange color. Sedimentary structures are difficult to find, and the rocks in general look rather highly oxidized and chemically altered. However, along the coastal exposures within and slightly above the intertidal zone at Punta San José, the beds are homoclinal and exhibit a dip to the west generally less than 10°, and are often exposed continuously along several kilometers of the coastline. The lower few meters of the exposed beds are in a reduced state, appearing as greenish mudstones which contain an abundance of fossils, charcoal fragments, amber and fibrous wood, pyrite concretions, and numerous sedimentary structures. From casts of wormholes, we deduce that the sediments were fairly actively bioturbated after deposition. We described, measured, and collected 99 oriented samples from a continuously exposed stratigraphic section over 110 m thick, composed of finely bedded to heavily bioturbated siltstone and clay siltstone. Occasional units within the sequence were composed of fine-grained, ripstone clast breccias with sharp upper and lower contacts and occasional exotic cobbles of crystalline rock 2–5 cm in diameter.

These units often contained fossil remains, including ammonites of the genus *Baculites*, and in the lower parts of the sequence, rare large (1–2 m) ammonites of the family *Baculites inornatus*. These large ammonites are thought to be restricted to Campanian time, which, according to the magnetic polarity time scale of *Harland et al.* [1982], implies that the sediments were probably deposited during the 6.5-m.y. long normal polarity chron 33N.

We also collected 21 oriented samples for a conglomerate test near the top of the sequence, from a poorly sorted ripstone and conglomerate bed. This unit was probably deposited in a regressive phase, and included large granitic cobbles, as well as large (>10 cm) bone fragments. The more highly oxidized state of these clasts, which had colored oxidation rims, indicated some possibility of a secondary chemoremanent magnetization.

Approximately 175 km to the southeast, the Maastrichtian Punta Baja formation [*Gastil*, 1975] is exposed along the coastline in a similar setting. Sediments of the Punta Baja formation are not as well preserved as El Rosario, but show a similar oxidation horizon in the exposed seacliffs. The beds occasionally show sulphurous accumulations, indicating the passage of groundwaters, and some possible elevated temperatures. We collected 32 oriented samples in a 10-m section within this unit.

SAMPLING TECHNIQUES

During the spring of 1983, and during several subsequent trips in 1984, we collected oriented samples for paleomagnetic analysis using standard gasoline powered drills, and oriented the cores with a clinometer and both magnetic and solar compasses when feasible, to an estimated accuracy of 2 degrees. We collected 152 oriented samples in stratigraphic sequence at two locations, one core per bed, with an average distance of 75 cm between cores. In the laboratory, we cut the cores into standard 2.5 cm paleomagnetic samples with a diamond saw, and washed them briefly in HCl to remove any metallic contaminants from the collection and preparation procedures. Measurements were made from one specimen per core.

All measurements of natural remanent magnetization (NRM) were taken on a two-axis superconducting magnetometer with a background noise below 10^{-11} Am^2 [*Goree and Fuller*, 1976; *Dunn and Fuller*, 1984]. This instrument is housed in a μ-metal shielded room with residual magnetic fields below 100 nT throughout most of the volume.

The cores were demagnetized with an initial alternating field (af) step of 5–7.5 mT to remove any viscous remanent components induced during sample collection or preparation. All af demagnetizations were performed on a semiautomatic three-axis Schonstedt demagnetization system. Pilot samples were run using a full af demagnetization sequence, but thermal demagnetization was chosen due to the large number of samples involved. Results are similar for the af and thermal demagnetizations.

Thermal demagnetizations were done in a large-volume, magnetically shielded furnace, using thermal steps of either 25 or 33 degrees, from 100°C to approximately 550°C, where magnetizations became unstable. Stable components of the NRM were isolated using principal component analysis [*Kirschvink*, 1980], and both *Bingham* [1974; *Onstott*, 1980] and *Fisher* [1953] statistics were used to estimate mean directions.

Chemical demagnetization using a concentrated solution of the reducing agent dithionate, $Na_2S_2O_4$, was also attempted. Severe degradation of the samples precluded any accurate determination of magnetization directions with this method.

Endchips from several samples at each locality were fully demagnetized with single-axis af, remagnetized with pulses of increasing field strength to give an acquired IRM (aIRM), and then demagnetized again using an af series to give the complementary curves in Figure 2. The shape of the isothermal remanent magnetism (IRM) versus field strength curve for each sample provides information on the mineralogy and magnetic particle size. The samples were measured along a single axis using the shielded magnetometer described previously.

Samples from both the reduced and oxidized facies were crushed and separated under acetone to prevent oxidation during crushing, and analyzed using room temperature Mössbauer spectroscopy to determine the ferric-ferrous ratio, and X-ray diffraction (XRD) to determine the mineralogy of the separates and residues. X-ray diffraction results were obtained with a Co-Kα source, using an Fe filter and a Debye-Scherrer camera. Intensities were calibrated by visual inspection, and correlated with files from the Mineral Powder Diffraction File [*Joint Committee on Powder Difraction Standards*, 1980]. Mössbauer results are all relative to a standard Fe foil calibration for isomer shifts.

IRM ACQUISITION RESULTS

Single-axis acquired isothermal remanent magnetization (aIRM) experiments were performed on endchips from all sites. The percentage of saturation IRM (sIRM) versus peak field of the demagnetizing af field or strength of the magnetizing pulse is shown in Figure 2 for four typical samples. Samples from locality PS2 behave essentially as those from PSJ, and BS2 behave as

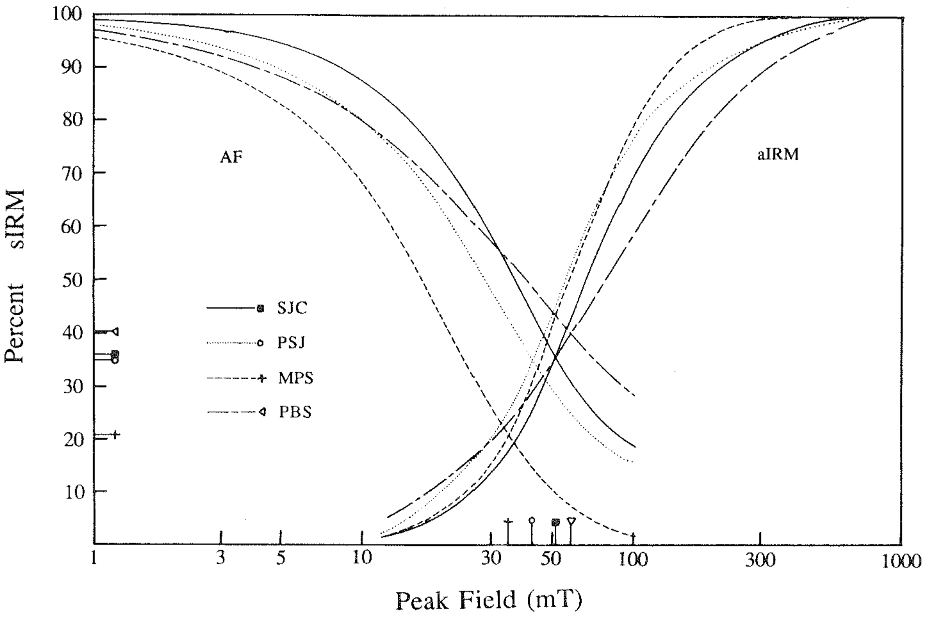

Fig. 2. Isothermal remanent magnetism (IRM) results for four localities. Percent saturation IRM is plotted versus peak magnetizing or demagnetizing field strength. Results for SJC, plotted as the solid curve, show a high initial coercivity indicating the presence of maghemite or goethite. All other sites display a soft demagnetization path characteristic of pseudosingle to single domain magnetite. The approximate remanent coercive field (H_{RC}) is indicated by the projection of the crossover point on the abscissa, and the ratio of the IRM at the crossover to the sIRM (R) is indicated by the projection onto the ordinate.

PBS. There are two main conclusions to be drawn from the results.

First, the low remanent coercive fields (H_{RC}) displayed by all the samples rule out hematite as the dominant magnetic mineral. Values for H_{RC} range from 34 mT for MPS to 59 mT for PBS. Hematite usually displays values for H_{RC} in the 1000 to 2000-mT range [*Roquet*, 1954*a*, *b*; *McElhinny*, 1973].

Second, the samples can be divided into two classes: a hard component that is demagnetized at relatively high peak af field strengths, which is found only in the San José conglomerate (SJC), and a softer component that is observed at all other sites. This result implies that the SJC sample has a different mineralogy from the other sites. The difference in the coercive field strength required to demagnetize the conglomerate sample could be due to the presence of more highly oxidized iron phases like maghemite or goethite. From the XRD and Mössbauer results that follow, we conclude that the magnetic particles in the SJC samples are distinct from those in the other samples, being both finer grained, and different mineralogically.

The majority of the samples show a behavior that is consistent with the presence of pseudosingle to single domain magnetite grains of submicron size [*Cisowski*, 1981]. Some measure of the grain interaction may be gained by looking at the ratio of the IRM at H_{RC} to the saturation IRM (R). Values of R range from 0.22 for MPS, indicating strong interaction, to 0.41 for PBS, indicating little interaction. Single domain grains are calculated to have relaxation times very much greater than 10^{11} years at room temperature [*Evans and MacElhinny*, 1969]. These types of grains can therefore maintain their magnetization for long periods, depending on the thermal history of the sediments. Because of the biochemical constraints, we conclude that the sediments have not been subjected to temperatures significantly affecting the relaxation time, and that the magnetization could well be primary.

X-RAY DIFFRACTION RESULTS

Extraction of magnetic minerals was attempted for both the reduced samples and the oxidized samples from the conglomerate test. Magnetic material was extracted from the reduced sample, as was expected from the large average magnetic moment for these samples, 1.02×10^{-7} Am^2. No visible magnetic phase was extracted from the oxidized samples, which had a much lower average moment of 1.01×10^{-8} Am^2.

A preliminary search in the Mineral Powder Diffraction File [*Joint Committee on Powder Diffraction Standards*, 1980] focused on a comparison with X-ray diffraction data for 11 magnetic mineral standard spectra, and 44 nonmagnetic spectra. The internal standard was provided by the quartz line at 3.343Å. Lines below 10% absorption were not included in the search.

The X-ray data are consistent with the possible presence of two minerals in the magnetic extract: magnetite and maghemite. The X-ray standard data for these minerals are, however, extremely similar, and although magnetite provides the best fit, with an average deviation of -0.0051Å versus 0.0089Å for maghemite, only Mössbauer spectroscopy could resolve them. We detected no magnetic minerals in the oxidized sample, even though the moment of the sample and its color indicated that at least a ferric oxide was present. The absence of X-ray diffraction lines, even when a mineral is known to be present, can occur with extremely small particle sizes, where Bragg diffraction becomes inefficient due to the small number of parallel lattice planes. X-ray diffraction can only confirm a mineral's presence, not discount it.

Nonmagnetic minerals present in all samples were quartz, potassic and sodic feldspars, micas, and their weathering products. Quartz and micas appear in the magnetic extracts, since these minerals are extremely hard to physically separate. The assemblage of feldspars, quartz, and weathered micas is the expected product of a granitic source.

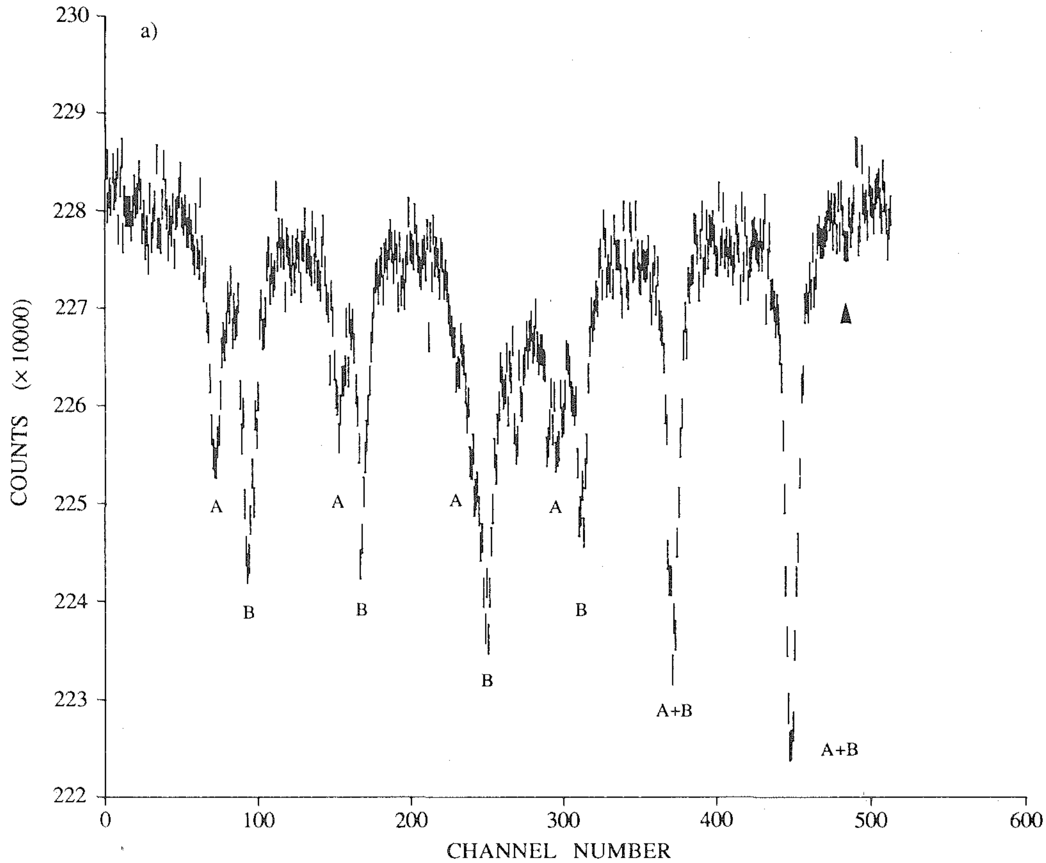

Fig. 3. Mössbauer spectra results for a magnetic extract, residue, and whole rock sample illustrating oxidation of the conglomerate bed. (*a*) Raw data plot of the Mössbauer spectrum from the magnetic extract of a reduced sample from the MPS locality. Points are plotted as counts read over a 2-day period, with one sigma standard deviation. Two sets of magnetic sextets are present, labeled A and B, along with some central peaks probably from Fe^{2+} in micas. Sextet series A and B result from the M1 and M2 sites in the inverse spinel structure of magnetite, with the characteristic peak height ratio of 1:2 from the stoichiometry of magnetite, $(Fe^{3+})(Fe^{3+},Fe^{2+})O_4$ the A peaks arising from the univalent tetrahedral site, and the B peaks from the divalent octahedral site. Maghemite has no Fe^{2+}, and would exhibit a peak height ratio of 1:1. Arrow indicates expected area for hematite peak. (*b*) Fitted Mössbauer spectrum for nonmagnetic residue left after matter producing spectrum of Figure 3*a* was extracted. Peaks are numbered as in Table 2. Isomer shift (δ) refers to the centerline of a peak pair, and quadrupole shift (Δ) to the separation between the pair, in millimeters per second. Peaks 1 and 5 are probably due to Fe^{3+} in a distorted M1 site, although the quadrupole shift value is high. Peaks 2 and 6 are due to Fe^{2+} in mica, and peaks 3 and 4 are due to Fe^{3+} in the M2 mica site, and possibly some iron oxide. The area of the peak is proportional to the amount of iron in that valence state and site. The Fe^{2+}/Fe^{3+} ratio for this spectrum fit is 56:44. (*c*) Fitted Mössbauer spectrum for a sample from the oxidized conglomerate bed. In comparison with Figure 3*b*, peaks 1 and 5, and 3 and 4 have all grown at the expense of peaks 2 and 6. This reflects the increasing oxidation of Fe^{2+} to Fe^{3+}. The Fe^{2+}/Fe^{3+} ratio for this spectrum fit is 32:68.

Mössbauer Results

Mössbauer spectra were obtained in two different velocity ranges for both the oxidized and reduced samples. The reduced sample was separated and analyzed as a magnetic and a residual fraction, as well as in whole rock form. The spectrum for the magnetic extract from a reduced sample from locality MPS at Punta San José in Figure 3*a* shows a typical magnetite sextet spectrum, along with some additional central ferrous peaks probably due to Fe^{2+} in mica sites. However, the most important detail is the peak height ratio of peaks A and B in the magnetic sextet. The A to B ratio of 1:2 for each pair is an indication that the magnetite in the reduced sample has not weathered appreciably to hematite or goethite. Magnetically ordered hematite should display a peak at an isomer shift higher than the highest combined A+B peak. While there is a small anomaly at a higher isomer shift, it contributes less than 2% of the total area. The isomer shift (δ) and quadrupole splitting (Δ) for magnetically ordered goethite are very similar to the A set, and would add to the area, reducing the 1:2 ratio. The amount of goethite here is less than 5%. The presence of magnetite, suggested by XRD, is confirmed, and maghemite (which would have an A:B of 1:1 at the same δ and Δ) is discounted.

The central features in the spectrum of the nonmagnetic residue from the reduced sample and the spectrum of the oxidized sample from the conglomerate test illustrate the change in oxidation state for iron. This is shown in Figures 3*b* and 3*c*, where the ferric peaks, 3 and 4, have grown more intense in the SJC sample at the expense of the ferrous peaks, 2 and 6, in the MPS residue sample. The MPS sample can be fit by a peak area ratio of 44% Fe^{2+} / 56% Fe^{3+}, while the oxidized SJC sample shows an increase in the ferric iron to 32% Fe^{2+} / 68% Fe^{3+}. The peaks 1 and 5 are probably due to ferric iron in a distorted M1 mica site, although the quadrupole shift for the MPS sample is somewhat anomalous.

The residual misfit in all these samples can be improved by adding further peaks due to several more lattice sites holding iron, albeit in much smaller quantities. However, the major

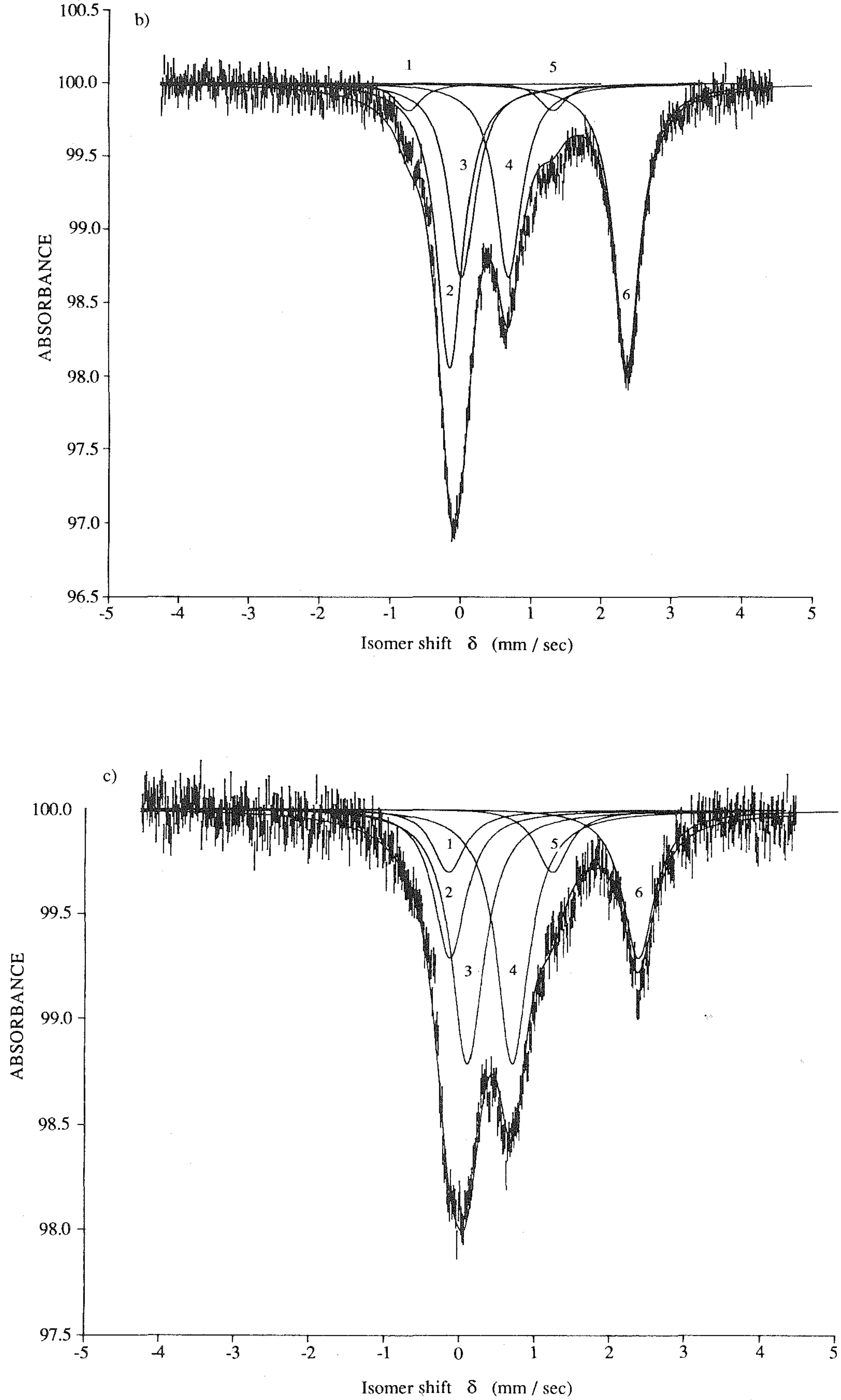

Fig. 3. (continued)

TABLE 2. Mössbauer Parameters

Peaks	δ mm/sec	Δ mm/sec	% Area	Source
		Reduced Residual Fraction		
1/5	0.2914 ± 0.0182	2.0605 ± 0.0367	5.528	Fe^{3+} (VI) distorted M1 mica site
2/6	1.1307 ± 0.0051	2.5496 ± 0.0061	56.142	Fe^{2+} (VI) distorted M1 mica site
3/4	0.3591± 0.0053	0.6660 ± 0.0060	38.328	Fe^{3+} (VI) regular M2 mica and Fe oxide
		Oxidized Conglomerate		
1/5	0.5335 ± 0.0111	1.3858 ± 0.0205	13.482	Fe^{3+} (VI) distorted M1 mica site
2/6	1.1296 ± 0.0059	2.5326 ± 0.0087	31.926	Fe^{2+} (VI) distorted M1 mica site
3/4	0.4026 ± 0.0058	0.8011 ± 0.0058	54.594	Fe^{3+} (VI) distorted M2 site and Fe oxide

δ, isomer shift relative to Fe foil standard; Δ, quadrupole splitting; % Area, integrated strength of fitted peak.

features of the spectra *have* been resolved, and it is not the intention of this paper to provide an exhaustive summary of the lattice sites containing iron.

The XRD experiment was not able to detect any magnetic minerals in the oxidized sample, and unfortunately, neither could the room temperature Mössbauer spectroscopy. The oxidized sample magnetic fraction is probably composed of extremely small particles, which could be identified only by cryogenic (4.2 K) spectroscopy. At this low a temperature goethite and hematite could be resolved even in very small particle sizes.

From these results we conclude that the samples from the greenish facies are relatively unweathered, and still contain magnetite, with no detectable goethite, hematite, or maghemite. The conglomerate test samples are much more highly oxidized, and their use as a test of magnetization can no longer be considered valid. The relevant Mössbauer parameters for the samples are presented in Table 2.

PALEOMAGNETIC RESULTS

Most of the samples analyzed in this study possessed a stable, univectorial magnetization which was easily recovered using principal component analysis. Samples with both normal and reversed polarities were collected, and include 99 normal samples at Punta San José (localities PSJ, MPS, and PS2), 32 mixed overprinted and (virtually) single-component reversed samples from Punta Baja (PBS), and 21 conglomerate test samples (SJC).

Zijderveld diagrams of typical samples from the Punta San José section show a linear demagnetization, with a component clearly intersecting the origin. Samples from Punta Baja show some single-component reversed samples, but a majority of reversed samples display a normal overprint. Samples from the conglomerate test show a unipolar distribution. However, in this case, Mössbauer spectroscopy indicates that the conglomerate has a different weathering history than the source bed. The

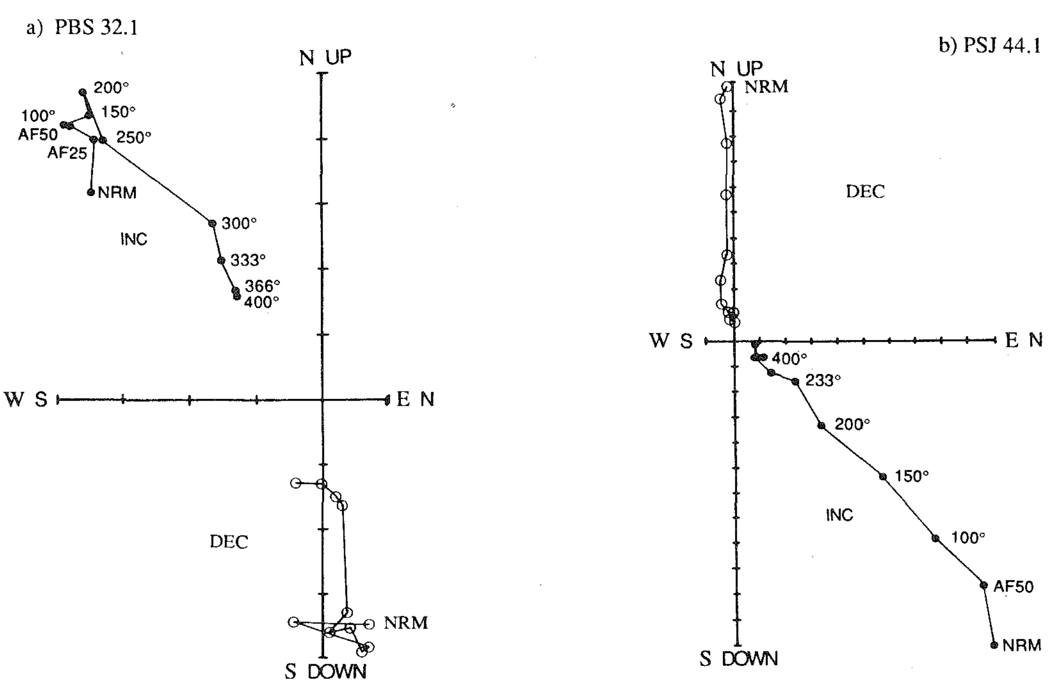

Fig. 4. Zijderveld diagrams for the thermal demagnetization of samples from Punta Baja and Punta San José. Dots indicate inclination relative to the vertical plane (UP–DOWN, N–S axes) for successive demagnetization steps, while open circles represent the corresponding declinations relative to the horizontal plane (N–S, E–W axes). Each division is 10^{-5} emu. Both samples are corrected for tilt of bedding. (*a*) Sample PBS 32.1 is representative of the reversed signal displayed by several samples collected at Punta Baja. (*b*) Sample PSJ 44.1 displays a univectorial normal signal, typical of all samples collected at Punta San José.

TABLE 3. Paleomagnetic Results by Site

Site	N	I	D	κ	α_{95}	VGPLat	VGPLong	Paleolat
				Punta San José (NRM Values)				
PS2	12	-39.8	192.9	9.4	13.1	-75.5	187.6	-22.6 ± 7.5
PSJ–A	20	40.6	3.7	17.0	8.2	81.2	40.7	23.2 ± 4.7
PSJ–B	20	50.3	-8.6	19.3	7.2	82.7	153.0	31.1 ± 5.2
PSJ–C	26	46.3	0.1	41.4	4.5	86.2	61.5	27.6 ± 2.9
MPS	21	55.7	20.2	5.9	14.3	72.6	311.9	36.2 ± 11.6
SJC*	21	47.2	10.5	14.9	8.5	80.4	349.2	28.3 ± 5.5
				Punta Baja (NRM Values)				
PBS	32	48.6	1.2	12.3	7.6	88.9	35.0	29.6 ± 5.2
Average NRM	131	46.6	3.5	11.8	3.7	85.3	21.8	29.0 ± 2.5
				Least Squares Fits				
PSJ	99	43.3	3.7	25.9	3.1	83.0	34.8	25.2 ± 1.9
PBS	32	-47.7	182.6	3.8	15.0	-87.5	180.4	-28.8 ± 10.2
Average	131	44.6	5.3	28.8	2.5	83.1	20.6	26.3 ± 1.6

Notation as in Table 1, along with VGPLat, VGPLong, virtual geomagnetic pole coordinates; averages are from Bingham fits to the NRM directions or least squares fits. All figures are corrected for the tilt of bedding.

* Figures for this site are not included in the average calculations.

choice of this particular conglomerate bed was inappropriate. The secondary component subparallel to the present field has been acquired by the oxidation products of magnetite. No control on the date of the oxidation was established, although the average declination of the samples, 10.5 ± 6.6°, indicates that there may have been some displacement since the time of oxidation. The Mössbauer results indicate that this set of samples has a CRM overprint. This overprint may not have been acquired during the same period as the primary magnetization, and so this set of samples was excluded from the mean pole calculation.

For an indication of the age of magnetization we rely on the reversed samples, along with the previously outlined biochemical and spectroscopic evidence for the lack of alteration. On thermal cleaning, samples from the Punta Baja section demonstrated either no overprint or a single present field overprint that left a stable, reversed endpoint. A reversed sample is illustrated in Figure 4. The results from this site are consistent with the Punta San José samples and show a reversed signal by 300°C.

To extract the normal and reversed components, 131 of 152 samples were used, and a least squares method was applied to the demagnetization vectors. These fits were then averaged with Bingham statistics. The resulting directions, shown in Table 3 and in Figure 5, are not very different from the Bingham statistics yielded by the raw NRM directions for 131 samples from the Punta San José and Punta Baja sites. All directions were corrected for the tilt of the bedding.

From Table 3 it can be seen that at the 95% confidence level, the paleolatitude implied by the NRM directions is the same as the paleolatitude from the least squares fits. This result is to be expected for univectorial magnetizations. The least squares directions from normal and reversed components were used in

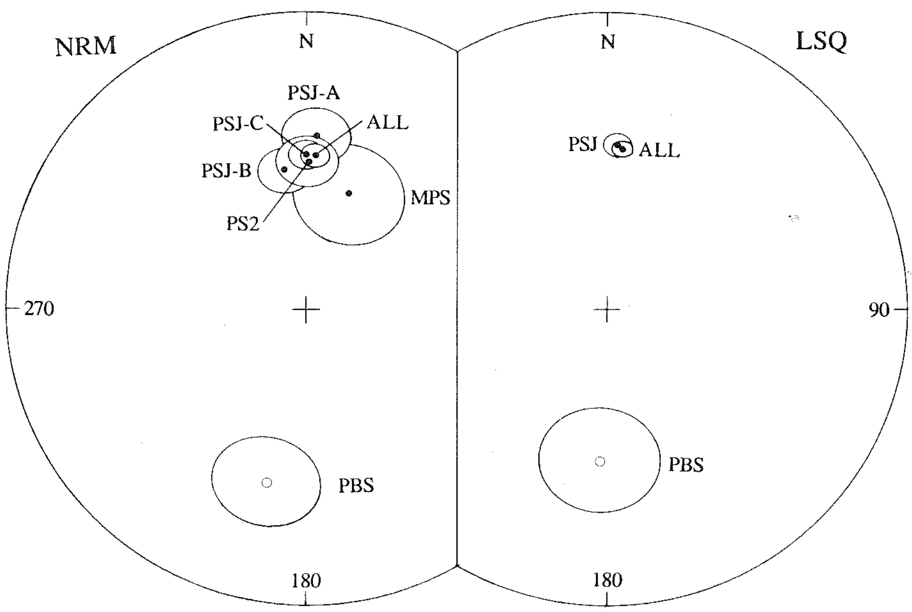

Fig. 5. Equal-area plots of the mean site directions and 95% confidence cones. NRM displays the initial magnetizations for each site, with site PBS displaying a reversed orientation, plotted with an open circle. LSQ displays the least squares analysis results for the two geographically separate sites, Punta San José, and Punta Baja. PSJ contains all sites near Punta San José except SJC. The cleaned, reversed component of PBS plots in the upper hemisphere. The label ALL indicates the Bingham analysis result for all the data within each of the plots.

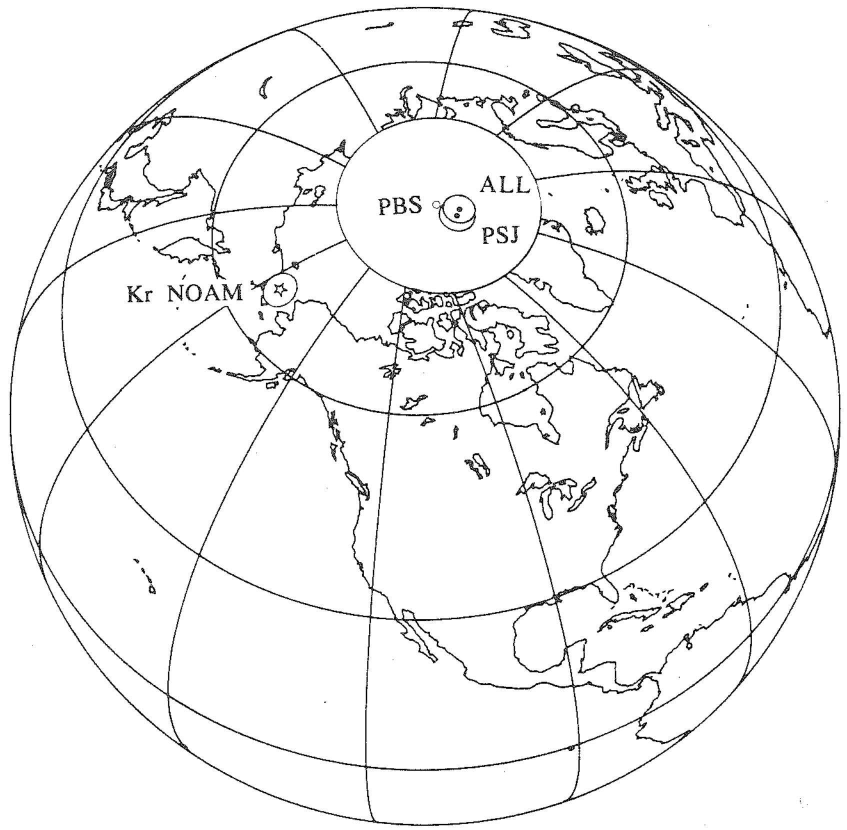

Fig. 6. Plot of the VGP positions for the least squares analysis. Star indicates the Cretaceous pole of *Irving and Irving* [1982], with an A_{95} of 3.4°. Open circle center symbol represents the reversed signature from the PBS site. ALL is the Bingham VGP for all the data from PSJ and PBS.

calculating the "average" values, and these therefore represent a mean direction for the peninsula during the times sampled.

Figure 6 illustrates the position of the virtual geomagnetic poles (VGP) for the two sites, along with the cones of 95% confidence. The 'ALL' VGP is the pole for all the least-square fits combined, including the reversed PBS pole, plotted with an open circle. The coincidence of these VGP's with the present location of the magnetic pole is purely accidental, since we have concluded that the magnetizations are indeed primary. The star indicates the location of the VGP for the North American craton, according to *Irving and Irving*'s [1982] moving window analysis of Cretaceous poles. The figures for displacement, d, and rotation, r, in Table 1 reflect the amount of motion required to bring these two poles into agreement, and suggest a 31° clockwise rotation and a 15° or 1670 ± 420 km poleward translation of the Baja Peninsula relative to the North American craton since the Campanian.

Discussion

This rock magnetic study revealed mineral grains of known geological stability in the pseudosingle to single domain region. The biochemical, IRM, X-ray, Mössbauer, and paleomagnetic data imply that the sediments at Punta San José have not been thermally or chemically altered. Under these constraints, we may virtually eliminate the possibility of chemical or thermal remagnetization. We conclude that the remanence is probably due to detrital or postdetrital remanent magnetization, the polarity of the samples being biased normal due to the 6.5-m.y. long normal interval in the Campanian. The Campanian age for the samples is supported by the presence of the fossil *Baculites inornatus*, and the younger reversed samples in sediments of Maastrichtian age. The younger samples from the Punta Baja formation have a normal overprint that is most likely a thermal component (TRM). We therefore conclude that the magnetization of the Punta San José sediments is primary, despite its similarity to the present axial dipole field, and that the reversed components detected in the Punta Baja sediments are also primary.

The mean magnetization direction for the sediments implies a paleolatitude of 26.3 ± 1.6°. At a 95% confidence level, this agrees with previous results obtained for Cretaceous rocks from the Baja California peninsula and the southern California area [*Patterson*, 1984; *Fry et al.*, 1985; *Hagstrum et al.*, 1985; *Champion et al.*, 1986]. This paleolatitude, when taken in conjunction with that of the of the North American craton, using the Cretaceous pole of *Irving and Irving* [1982], implies that the peninsula has moved approximately 1670 ± 420 km northwards relative to the North American craton since the Cretaceous, at an average velocity of at least 16 mm/year. Data from Miocene volcanic rocks on the peninsula show no diplacement, indicating that the peninsula was adjacent to the Mexican mainland before the opening of the gulf of California at least by the early Miocene [*Bobier and Robin*, 1983; *Hagstrum et al.*, 1987]. This implies that the peninsula moved northwards with at least an average velocity of 19 mm/year. These velocities are within the allowed error of plate reconstruction models involving the North American, Pacific, and Farallon plates [*Hagstrum et al.*, 1985].

Shallow inclinations can be caused by reasons other than low paleolatitudes. Magnetic inclination shallowing during sediment compaction has been ruled out by the collection of data from sedimentary and plutonic rocks on the peninsula which show similar results [*Hagstrum et al.*, 1985] as well as the consistency from site to site within all data sets. The presence of higher order moments in the field, expressed as secular variations, has also been discounted, since the Cretaceous and Miocene results for the rest of the North American craton give good agreement with a dipole dominated field [*Irving and Irving*, 1982]. The opening of the Gulf of California can account for only 2° of the translation, and 8° of the rotation [*Larson*, 1972]. Results from the mainland, in an older sequence of andesitic lavas and batholithic granodiorites ranging in age from 45 to 100 Ma [*McDowell and Keizer*, 1977; *McDowell and Clabaugh*, 1979] beneath the Miocene rhyolites of the Sierra Madre Occidental in Sinaloa, also show a low paleolatitude, indicating that motion in the Paleogene included some terranes to the east of the Gulf [*Hagstrum et al.*, 1987]. In fact, the presence of this mainland data may provide a hypothesis for the resolution of the current conflict between the geological and paleomagnetic communities regarding the motion of the Baja California peninsula. If the northwestward motion also included parts of the mainland, as suggested by the presence of several right-lateral strike-slip faults mapped by *Gastil and Krummenacher* [1977], the correlation of Late Cretaceous to early Tertiary units across the Gulf does not conflict with the paleomagnetic data. Data from geochemical studies, however, would seem to indicate that the magmatic activity producing the Peninsular Ranges Batholith migrated to the east across the plate margin without offset, reaching Sonora by the Paleocene [*Anderson et al.*, 1969; *Silver et al.*, 1969; *Silver*, 1986].

It is clear that paleomagnetic work on the mainland, specifically in areas near and to the east of the fault lineaments would provide a clearer picture of the timing and locus of the movement of the Peninsula. A clear compilation of the constraints on the motion of the peninsula is sorely needed, with collaboration from the paleomagnetic, geological, and geochemical communities. The boundary along which the motion occurred may have jumped several times, an effect observed between the San Andreas and the San Gabriel Faults in southern California. The change in active fault location, along with the sparse nature of the collected data, makes interpretation of the motion difficult, and may lead one to impose a large-scale constraint, when in fact the constraint may strictly only be applicable locally.

The coastal area in question was a right-lateral oblique subduction zone during the Cretaceous and early Tertiary. From the amount of displaced terranes detected in the much better sampled areas of California, we should expect to find similar complexity in an area experiencing maximum convergence between the North American and Farallon plates during precisely latest Cretaceous and early Tertiary times [*Engebretson*, 1983].

Acknowledgments. This work was supported by the Caltech Summer Undergraduate Research Fund Program (SURF-83), NSF grant EAR83-51370 (JLK), and an NSF graduate fellowship (PEF). The authors wish to thank Roger Burns for the use of the XRD and Mössbauer instruments, while Heinz A. Lowenstam, Leon T. Silver, and Jan Smit provided guidance with fossil identification, sampling localities, and biostratigraphy. Roger Burns and Teresa Solberg provided fruitful discussion of the XRD and Mössbauer data. The authors also wish to thank J. Hagstrum and an anonymous reviewer for their highly constructive comments. Caltech Geological and Planetary Sciences contribution number 4672.

REFERENCES

Anderson, T. H., L. T. Silver, M. Córdoba, and A. Diego, Mesozoic magmatic events of the Northern Sonora coastal region, Mexico (abstract), *Geol. Soc. Am. abstr. Programs*, *7*, 3–4, 1969.

Bada, J. L., and R. A. Schroeder, Racemization of isoleucine in calcareous marine sediments: Kinetics and mechanism, *Earth Planet. Sci. Lett.*, *15*, 1–11, 1972.

Bathurst, R. G. C., *Carbonate Sediments and Their Diagenesis*, 2nd ed., 685pp., Elsevier Science, New York, 1975.

Beck, M. E., Jr., and P. W. Plumley, Late Cenozoic subduction and continental-margin truncation along the northern Middle America Trench: Discussion, *Geol. Soc. Am. Bull.*, *90*, 792–794, 1979.

Bingham, C., An antipodally symmetric distribution on a sphere, *Ann. Stat.*, *2*, 1201–1225, 1974.

Bischoff, J. L., and W. S. Fyfe, Catalysis, inhibition, and the aragonite–calcite transformation, *Am. J. Sci.*, *266*, 65–79, 1968.

Bobier, C., and C. Robin, Paléomagnetisme de la Sierra Madre Occidentale dans les états de Durango et Sinaloa (Mexique): Variations du champ ou rotations de blocs au Paleocène et au Neogène, *Geofís. Int.*, *22*, 57–86, 1983.

Bøggild, O. P., The shell structure of the molluscs, *Kgl. Vidensk. Selsk. Skr. Naturv. Mat.*, *9*(33), 1–15, 1930.

Brand, U., and J. O. Morrison, Paleoscene #6: Biogeochemistry of fossil marine invertebrates, *Geosci. Can.*, *14*(2), 85–107, 1987.

Champion, D. E., D. G. Howell, and C. S. Grommé, Paleomagnetic and geologic data indicating 2500 km of northward displacement for the Salinian and related terranes, California, *J. Geophys. Res.*, *89*, 7736–7752, 1984.

Champion, D. E., D. G. Howell, and M. Marshall, Paleomagnetism of Cretaceous and Eocene strata, San Miguel Island, California Borderland and the northward translation of Baja California, *J. Geophys. Res.*, *91*, 11557–11570, 1986.

Cisowski, S., Interacting vs. non–interacting single domain behavior in natural and synthetic samples, *Phys. Earth Planet. Inter.*, *26*, 56–62, 1981.

Curtis, C. D., and D. Krinsley, The detection of minor diagenetic alteration in shell material, *Geochim. Cosmochim. Acta*, *29*, 71–84, 1965.

Dunn, J. R., and J. M. Fuller, Thermal demagnetization with measurement at high temperature using a SQUID magnetometer (abstract), *Eos Trans. AGU*, *65*, 863, 1984.

Engebretson, D. C., Relative motions between the North American, Kula, Farallon, and Pacific plates from 145 My to the present, Ph.D. thesis, 211 pp., Stanford Univ., Stanford, Calif., 1983.

Evans, M. E., and M. W. McElhinny, An investigation of the origin of stable remanence in magnetite bearing igneous rocks, *J. Geomagn. Geoelectr.*, *21*, 757–773, 1969.

Fisher, R. A., Dispersion on a Sphere, *Proc. R. Astron. Soc. of London, Ser. A*, *217*, 295–305, 1953.

Fry, J. G., D. J. Bottjer, and S. P. Lund, Magnetostratigraphy of displaced upper Cretaceous strata in southern California, *Geology*, *13*, 648–651, 1985.

Gastil, R. G., and D. Krummenacher, Reconnaissance geology of coastal Sonora between Puerto Lobos and Bahía Kino, *Geol. Soc. Am. Bull.*, *88*, 189–198, 1977.

Gastil, G., G. J. Morgan, and D. Krummenacher, The tectonic history of peninsular California and adjacent Mexico, in *The Geotectonic development of California*, edited by W.G. Ernst, pp. 2–28, Prentice-Hall, Englewood Cliffs, N. J., 1981.

Gastil, R. G., R. P. Phillips, and E. C. Allison, Reconnaissance geology of the state of Baja California, *Mem. Geol. Soc. Am.*, *140*, 1–170, 1975.

Goree, W. S., and J. M. Fuller, Magnetometers using RF driven SQUIDs and their applications in rock magnetism and paleomagnetism, *Rev. Geophys.*, *14*, 591–608, 1976.

Hagstrum, J. T., M. McWilliams, D. G. Howell, and S. Grommé, Mesozoic paleomagnetism and northward translation of the Baja California Peninsula, *Geol. Soc. Am. Bull.*, *96*, 1077–1090, 1985.

Hagstrum, J. T., M. G. Sawlan, B. P. Hausback, J. G. Smith, and C. S. Grommé, Miocene paleomagnetism and tectonic setting of the Baja California Peninsula, Mexico, *J. Geophys. Res.*, *92*, 2627–2639, 1987.

Hare, P. E., and P. H. Abelson, Racemization of amino-acids in fossil shells, *Year Book Carnegie Inst.*, *66*, 526–528, 1968.

Harland, W. B., A. V. Cox, P. G. Llewellyn, C. A. G. Pickton, A. G. Smith, and R. Walters, *A Geologic Time Scale*, 131 pp., Cambridge University Press, New York, 1982.

Irving, E., and G. A. Irving, Apparent polar wander paths, Carboniferous through Cenozoic and the assembly of Gondwana, *Geophys. Surv.*, *5*, 141–188, 1982.

Jackson, T. A., and J. L. Bischoff, The influence of amino acids on the kinetics of the recrystallization of aragonite to calcite, *J. Geol.*, *79*, 493–497, 1971.

Joint Committee on Powder Diffraction Standards, *Mineral Powder Diffraction File*, 1168 pp., International Centre for Diffraction Data, Swarthmore, Pa., 1980.

Kilmer, F. H., *Late Cretaceous stratigraphy and paleontology, El Rosario, Northwestern Baja California, Mexico*, pp. 31–32, Geological Society of America, Cordilleran Section, Fresno, Calif., 1965.

Kirschvink, J. L., The least squares line and plane analysis of paleomagnetic data, *Geophys. J. R. Astron. Soc.*, *62*, 699–718, 1980.

Larson, R. L., Bathymetry, magnetic anomalies, and plate tectonic history of the mouth of the Gulf of California, *Geol. Soc. Am. Bull.*, *83*, 3345–3360, 1972.

McDowell, F. W., and S. E. Clabaugh, Ignimbrites of the Sierra Madre Occidental and their relation to the tectonic history of western Mexico, *Spec. Pap. Geol. Soc. Am.*, *180*, 113–124, 1979.

McDowell, F. W., and R. P. Keizer, Timing of mid-Tertiary volcanism in the Sierra Madre Occidental between Durango City and Mazatlan, Mexico, *Geol. Soc. Am. Bull.*, *88*, 1479–1487, 1977.

McElhinny, M. W., *Paleomagnetism and Plate Tectonics*, 358 pp., Cambridge University Press, New York, 1973.

McWilliams, M. O., and D. G. Howell, Exotic terranes of Western California, *Nature*, *297*, 215–217, 1982.

Onstott, T. C., Application of the Bingham distribution function in paleomagnetic studies, *J. Geophys. Res.*, *85*, 1500–1510, 1980.

Page, B. M., The southern Coastal Ranges, in *The Geotectonic Development of California*, edited by W.G. Ernst, pp. 329–417, Prentice-Hall, Englewood Cliffs, N. J., 1981.

Patterson, D. L., Paleomagnetism of the Valle Formation and late Cretaceous paleogeography of the Vizcaino Peninsula basin, Baja California, Mexico, in *Geology of the Baja California Peninsula*, edited by V.A. Frizell, Jr., pp.173–183, Society of Economic Paleontologists and Mineralogists, Pacific Coast Section, Bakersfield, Calif., 1984.

Roquet, J., Sur les remanences des oxydes de fer et leur interêt en géomagnetisme, *Ann. Geophys.*, *10*, 226–247, 1954*a*.

Roquet, J., Sur les remanences des oxydes de fer et leur interêt en géomagnetisme, *Ann. Geophys.*, *10*, 282–325, 1954*b*.

Silver, L. T., Observations on the Peninsular Ranges Batholith, southern California and Mexico, in space and time (abstract), *Geol. Soc. Am. Abstr. Programs*, *18*, 184, 1986.

Silver, L. T., C. R. Allen, and F. G. Stehli, Some petrological, geochemical, and geochronological observations of the Peninsular Range Batholith of northwestern Baja California, Mexico, *Spec. Pap. Geol. Soc. Am.*, *121*, 279–280, 1969.

Strangway, D. W., B. E. McMahon, T. R. Walker, and E. E. Larson, Anomalous Pliocene paleomagnetic pole positions from Baja California, *Earth Planet. Sci. Lett.*, *13*, 161–166, 1971.

Teissère, R. F., and M. E. Beck, Jr., Divergent Cretaceous paleomagnetic pole positions for the Southern Califiornia Batholith, USA, *Earth Planet. Sci. Lett.*, *18*, 296–300, 1973.

Weiner, S., and H. A. Lowenstam, Well preserved fossil mollusk shells: Characterization of mild diagenetic processes, in *Biogeochemistry of Amino Acids*, edited by P.E. Hare, pp. 95–114, John Wiley and Sons, New York, 1980.

Weiner, S., H. A. Lowenstam, B. Taborek, and L. Hood, Fossil mollusk shell organic matrix components preserved for 80 million years, *Paleobiology*, *5*, 144–150, 1979.

P.E. Filmer, Department of Earth, Atmospheric, and Planetary Sciences, 54-810 MIT, 77 Massachusetts Avenue, Cambridge, MA 02139.

J.L. Kirschvink, Division of Geological and Planetary Sciences, California Institute of Technology, Pasadena, CA 91125.

(Received August 29, 1988;
revised February 17, 1989;
accepted February 28, 1989.)